DESY 95-002
January 1995

Higgs and Background Production in the Reaction $e^+e^- \longrightarrow b\bar{b} + 2$ Jets at LEPII and NLC Energies

E. Boos

Deutsches Elektronen-Synchrotron DESY
Institut für Hochenergiephysik IfH, Zeuthen

and

Nuclear Physics Institute, Moscow State University, Russia

M. Sachwitz, H. J. Schreiber

Deutsches Elektronen-Synchrotron DESY
Institut für Hochenergiephysik IfH, Zeuthen

S. Shichanin

Deutsches Elektronen-Synchrotron DESY
Institut für Hochenergiephysik IfH, Zeuthen

and

Institute for High Energy Physics, Protvino, Moscow Region, Russia

ISSN 0418-9833

DESY 95- 002
January 1995

ISSN 0418-9833

Higgs and Background Production in the Reaction $e^+e^- \longrightarrow b\bar{b}$ + 2 jets at LEPII and NLC Energies

E. Boos[1,2], M. Sachwitz[1], H. J. Schreiber[1] and S. Shichanin[1,3]

[1]DESY-Institut für Hochenergiephysik, Zeuthen, FRG
[2]Nuclear Physics Institute, Moscow State University, 119899, Moscow, Russia
[3]Institute for High Energy Physics, 142284, Protvino, Moscow Region, Russia

Abstract

A complete tree-level Standard Model calculation of the reaction $e^+e^- \longrightarrow b\bar{b}$ + 2 jets in the energy range of LEPII and the Next e^+e^- Linear Collider is presented. The 2-jet system represents either a $q\bar{q}$ pair or two gluons. The matrix elements were calculated by means of the package CompHEP, and phase space integration and event generation were carried out with the computer programs BASES/SPRING. Cross sections of the Higgs boson, the total background and important subsets of background are studied as functions of the c.m.s. energy and the Higgs mass, taking into account possible interferences. Various event distributions calculated for realistic integrated luminosities indicate encouraging prospects regarding the extraction of the Higgs signal.

1 Introduction

One of the most important problems in today's elementary particle physics is the understanding of the origin of the masses of the particles. In the Standard Model (SM) the fundamental particles receive masses through the interaction with a scalar field [1] which corresponds to a real physical neutral scalar particle, the Higgs boson H^0. The Higgs mass is however not predicted by the SM and experiments which have searched for it set a lower limit of $M_H \simeq 64.5$ GeV, see e.g. ref. [2]. If the mass of the Higgs boson is $\lesssim$140 GeV, the SM predicts its main decay being to b and $\bar{b}$ quarks, $H^0 \longrightarrow b\bar{b}$, in about 85% of the cases. Thus a very promising reaction for its detection and the study of its properties is

$$e^+e^- \longrightarrow b\bar{b} + 2 \text{ fermions} \tag{1}$$

at LEPII and Next e^+e^- Linear Collider (NLC) energies [3]. It is expected that the main production mechanisms for the Higgs in reaction (1) are the Higgsstrahlung off the Z boson [4]

$$e^+e^- \longrightarrow H^0 Z \tag{2}$$

with the decays

$$Z \longrightarrow l\bar{l} \quad (l = e, \mu, \tau, \nu_e, \nu_\mu, \nu_\tau) \quad \text{or} \quad Z \longrightarrow q\bar{q} \quad (q = u, d, s, c, b)$$

and the fusion process [5]

$$e^+e^- \longrightarrow H^0\, l\bar{l} \qquad (l = e, \nu_e). \tag{3}$$

In several studies of reaction (1) at LEPII and NLC energies, discovery potentials for the Higgs boson were estimated [6, 7, 8]. Some questions have

however remained unanswered and should be discussed, in particular, questions like how large are the contributions from non-leading diagrams and to what extent are interferences expected to influence the Higgs signal and its properties. For the particular cases that the fermion in reaction (1) is a muon, a neutrino or an electron such detailed studies based on complete tree-level calculations have been carried out. The reaction

$$e^+e^- \longrightarrow b\bar{b}\ \mu^+\mu^- \tag{4}$$

turned out to have the cleanest signature for the Higgs but the event rate is rather small [9, 10]. Six times more Higgs events are expected in the reaction

$$e^+e^- \longrightarrow b\bar{b}\ \nu\bar{\nu}, \tag{5}$$

to which some extra contribution arises from the fusion process (3) at energies above LEPII [11, 12]. The reaction

$$e^+e^- \longrightarrow b\bar{b}\ e^+e^- \tag{6}$$

turned out to be the most complicated one from the calculational point of view, and the extraction of the Higgs signal out of a background that is two orders of magnitude larger, requires well designed cuts [13].

In the energy range of LEPII and NLC (for which, in its first stage of development, a c.m.s. energy of $\sqrt{s} = 300$ GeV is anticipated) the Higgsstrahlung process (2) dominates. Most of the events are expected to contain, besides the b and $\bar{b}$ quark jets from the Higgs, two additional jets from the dominat $Z \longrightarrow q\,\bar{q}$ decay. Thus, from a statistical point of view, events with a 4-jet topology (two of them being identified as b quarks by dedicated vertex detectors) account for about 60% of all H^0 events produced in reaction (2).

The aim of this paper is to investigate Higgs production, and the detection potential for Higgs, in the reaction

$$e^+e^- \longrightarrow b\bar{b} + 2\ \text{jets} \tag{7}$$

in competition with the large expected background, by taking into account the complete set of tree-level diagrams as well as possible interference terms. The rate for reaction (7) is given by the sum of the rates for the channels

$$e^+e^- \longrightarrow b\bar{b}\ q\bar{q}, \tag{8}$$

with the symbol q denoting the sum over the u, d, s, c and b quark states, and

$$e^+e^- \longrightarrow b\bar{b}\ gg. \tag{9}$$

Some of these reactions have been considered in ref. [14] and most of the results have been presented for LEPI energies. In a recent paper [15] some of the possible diagrams (the electroweak tree-level diagrams only) were used to calculate cross sections for the production of four massless quarks. It has been found that these results are in good agreement with semi-analytical calculations [16]. In particular, for the subchannel $e^+e^- \longrightarrow W^+W^-$, with subsequent $W \longrightarrow q\bar{q}$ decays, encouraging agreement has been observed [17]. Independently, gluonic background due to $e^+e^- \longrightarrow g\,g + q\,\bar{q}$ [18] has been added to the 4-quark final state calculations of ref. [15]. However, no complete and thorough study of reaction (7) exists which is particularly important for the Higgs search in an energy range of $\sqrt{s} =$ 160 - 500 GeV and for Higgs masses in the intermediate range M_H = 80 - 140 GeV.

In order to impose a 4-jet final state event topology and to avoid at the same time some of the singularities in the matrix elements, we require for each pair of partons the invariant mass and the opening angle to fulfill the conditions

$$M_{ij} > 10 \text{ GeV} \qquad \text{and} \qquad |\cos\Theta_{ij}| < 0.9, \tag{10}$$

respectively. These conditions were also applied in refs. [15, 18]. Furthermore, we assume a 100% efficiency for b-tagging in our calculations. Thus, cross section values and event distributions presented in this paper are subject to these restrictions.

The paper is organized as follows. In sect. 2 total cross sections for reaction (7) as well as the breakdown into the main components (reaction (8), reaction (9) and reaction (2)) are discussed. The method of calculation and the input parameters are described as well. Sect. 3 is devoted to a detailed study of Higgs production, in particular its dependence on the c.m.s. energy and its mass. In sect. 4 different background contributions and their relative weights are discussed. Attention is directed to possible interference contributions. In sect. 5 the extraction of the Higgs signal out of the 4-jet background rate is presented. Sect. 6 contains the summary and conclusions.

2 The cross section of the reaction $e^+e^- \longrightarrow b\,\bar{b}$ + 2jets and the Higgs signal rate

The calculation of the cross section for reaction (7) which includes the Higgs production process (2) as a subchannel, with $H^0 \longrightarrow b\,\bar{b}$ and $Z \longrightarrow q\,\bar{q}$ decays, has been performed in the same manner as for reactions (4) - (6) in refs. [10, 11, 13]. The procedure consists of two main steps. The generation of Feynman diagrams, the analytical expressions for the matrix elements squared and the corresponding optimized Fortran codes have been obtained by means of the computer package CompHEP [19]. The integration over phase space and the

generation of the event flow have been done with the help of the adaptive Monte Carlo integrator BASES/SPRING [20]. It is worth emphasizing that because of the complicated phase space structure of the 4-fermion final states and the occurence of singularities, a reasonable choice of variables and smoothing of singularities were mandatory. Today's version of CompHEP offers all the features needed to overcome these problems [21].

Our calculations include Breit-Wigner propagators for the Higgs and Z bosons, the tree-level Higgs width and the following set of parameters: $M_Z = 91.16$ GeV, $\Gamma_Z = 2.53$ GeV, $\alpha = 1/128$, $\alpha_s = 0.115$, $\sin^2\Theta_W = 0.226$, $M_W = M_Z \cos\Theta_W$, $m_b = 5$ GeV, $m_c = 1.35$ GeV, $m_s = 0.130$ GeV, $m_u = m_d = 0$ and $V_{cb} = 0.044$. The t'Hooft-Feynman gauge is used. Unphysical ghosts and Goldstone contributions, which appear as an internal property in this gauge, are included in the cross section calculations.

All lowest order diagrams contributing to reaction (7) are collected in Figs. 1 and 2. Ghost and Goldstone diagrams are not shown in these figures. Fig. 1 contains all $b\bar{b} + q\bar{q}$ final state diagrams which are either of pure electroweak or electroweak-QCD nature. Fig. 2 shows the diagrams contributing to reaction (9), $e^+e^- \longrightarrow b\bar{b} + 2$ gluons. Interferences between the diagrams are expected only

- within a given class of diagrams, i.e. either between the electroweak or the electroweak-QCD diagrams in Fig. 1 or between those in Fig. 2,

and

- between the electroweak and electroweak-QCD diagrams of Fig. 1 only in cases of $q = b$ and $\bar{q} = \bar{b}$.

In our calculations these interference terms were generally taken into account. Only in those cases explicitely stated, they have been neglected because of their very small sizes. It is also worth pointing out that the subprocesses mentioned so far are gauge invariant by themself, so that their cross sections can be calculated and compared with each other.

In Fig. 3 the total cross section for the reaction $e^+e^- \longrightarrow b\bar{b} + 2$ jets is presented as a function of $\sqrt{s}$ between 160 and 500 GeV (full curve). We also show in this figure the cross sections for the Higgs signal (with $M_H = 80$ GeV) and the background contributing to reaction (8) as well as the total cross section for reaction (9).

As can be seen the total event rate close to $\sqrt{s} = 160$ GeV is dominated by the 2-gluon final state which decreases as $1/s$ with increasing energy and is found to be the most important contribution above $\sqrt{s} \sim 300$ GeV. The $b\bar{b} + q\bar{q}$ background part does not exceed 15% of the total rate at $\sqrt{s} \leq 170$ GeV. The sharp rise of the overall reaction (7), $e^+e^- \longrightarrow b\bar{b} + 2$ jets, between $\sqrt{s} \approx$

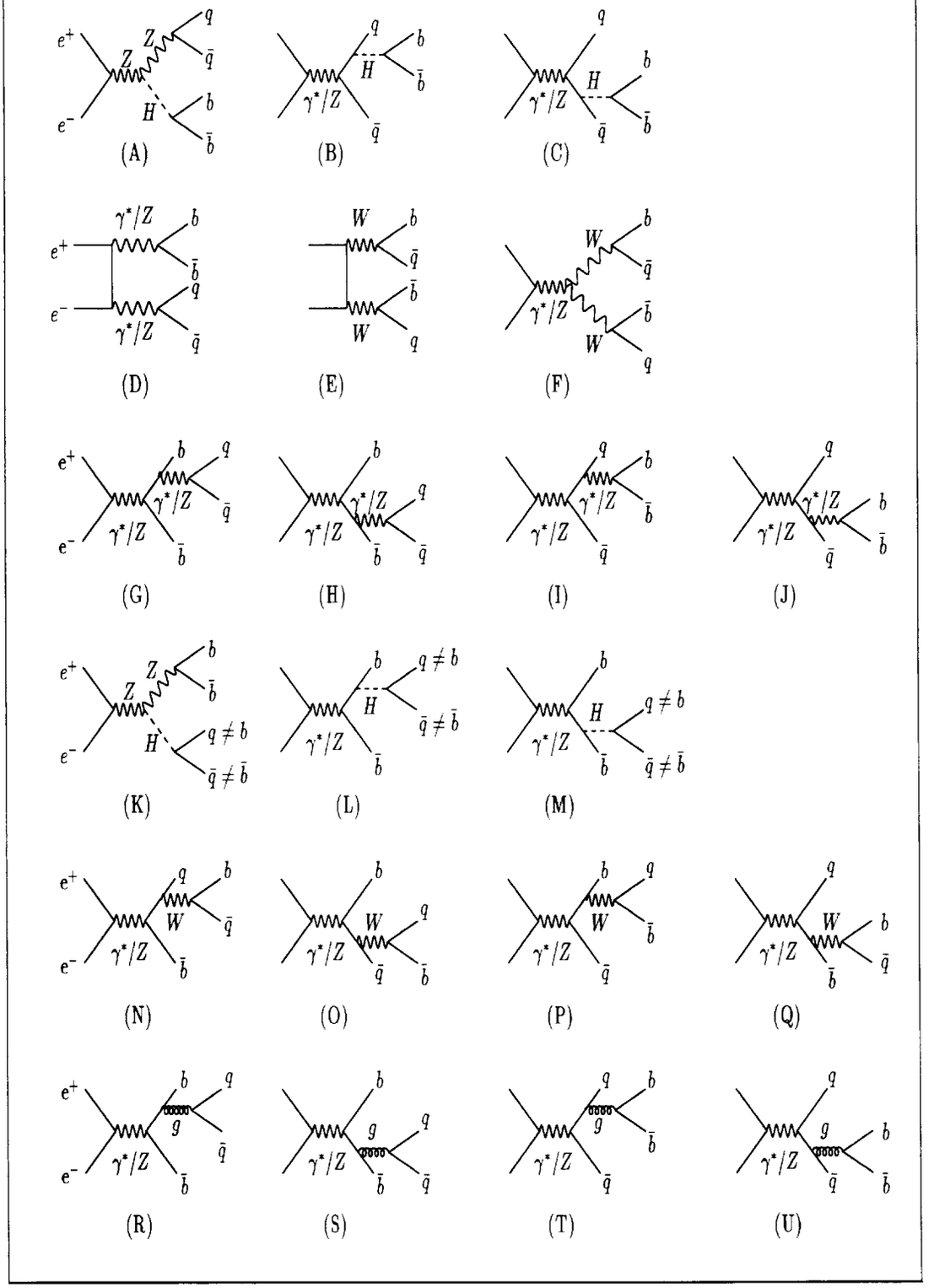

Figure 1: Tree-level diagrams contributing to the reaction $e^+e^- \longrightarrow b\bar{b} + q\bar{q}$.

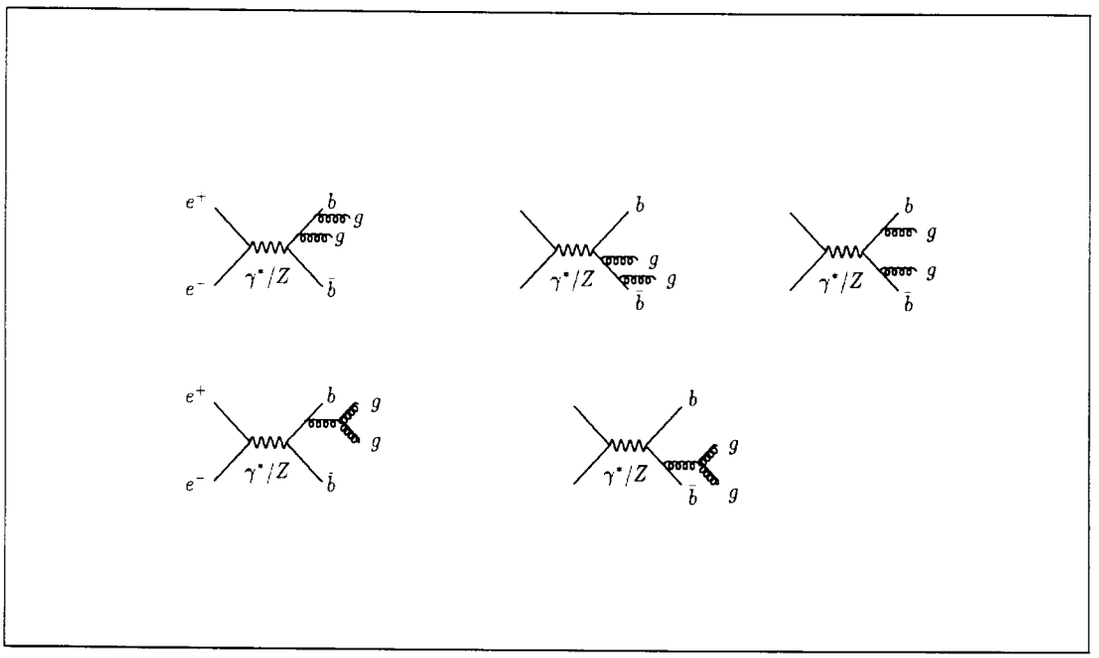

Figure 2: Tree-level diagrams contributing to the reaction $e^+e^- \longrightarrow b\bar{b}$ + 2 gluons.

170 GeV and 200 GeV is due to the onset of the Higgs production (dashed curve) and the two-body reaction $e^+e^- \longrightarrow ZZ$, with the subsequent decays of $Z \longrightarrow b\bar{b}$ and $Z \longrightarrow q\bar{q}$, which dominates the total $b\bar{b} + q\bar{q}$ background event rate. Somewhat above 200 GeV, these cross sections decrease with increasing energy so that at $\sqrt{s} \geq 300$ GeV the 2-gluon contribution dominates again. In the energy region of LEPII ($\sqrt{s} \simeq 190$ - 200 GeV), the H^0 rate (with $M_H =$ 80 GeV) contributes about 40% to the total $b\bar{b}$ + 2 jets event rate, whereas at $\sqrt{s} = 500$ GeV it is one order of magnitude lower.

3 The Higgs boson signal

As shown in Fig. 1 there are two different types of diagrams responsible for Higgs production. Diagram (A) represents the Higgsstrahlung off the Z boson with subsequent $H^0 \longrightarrow b\bar{b}$ and $Z \longrightarrow q\bar{q}$ decays, while diagrams (B) and (C) correspond to Higgs radiation off a quark, with $H^0 \longrightarrow b\bar{b}$ decay in a second step. Since the Higgs couplings to the u, d, s and c quarks are small in the SM, only the diagram with Higgsstrahlung off the b quark may be important. Our estimations for Higgs radiation off a b quark revealed, for example, 1.3 10^{-3} fb at $\sqrt{s} = 200$ GeV and $M_H = 80$ GeV, and 2.9 10^{-4} fb at $\sqrt{s} = 300$ GeV and $M_H = 140$ GeV, and interferences between the Higgs production diagrams were also found to be negligible. Thus, only Higgsstrahlung off the Z boson is important, and its rate as a function of energy is shown in Fig. 4 for several Higgs masses, $M_H = 80$, M_Z, 100, 120 and 140 GeV, summed over all $Z \longrightarrow q\bar{q}$ decays. The behaviour of these distributions is analogous to those obtained for the leptonic Z decays [10]-[13]: they rise sharply near threshold, reach a

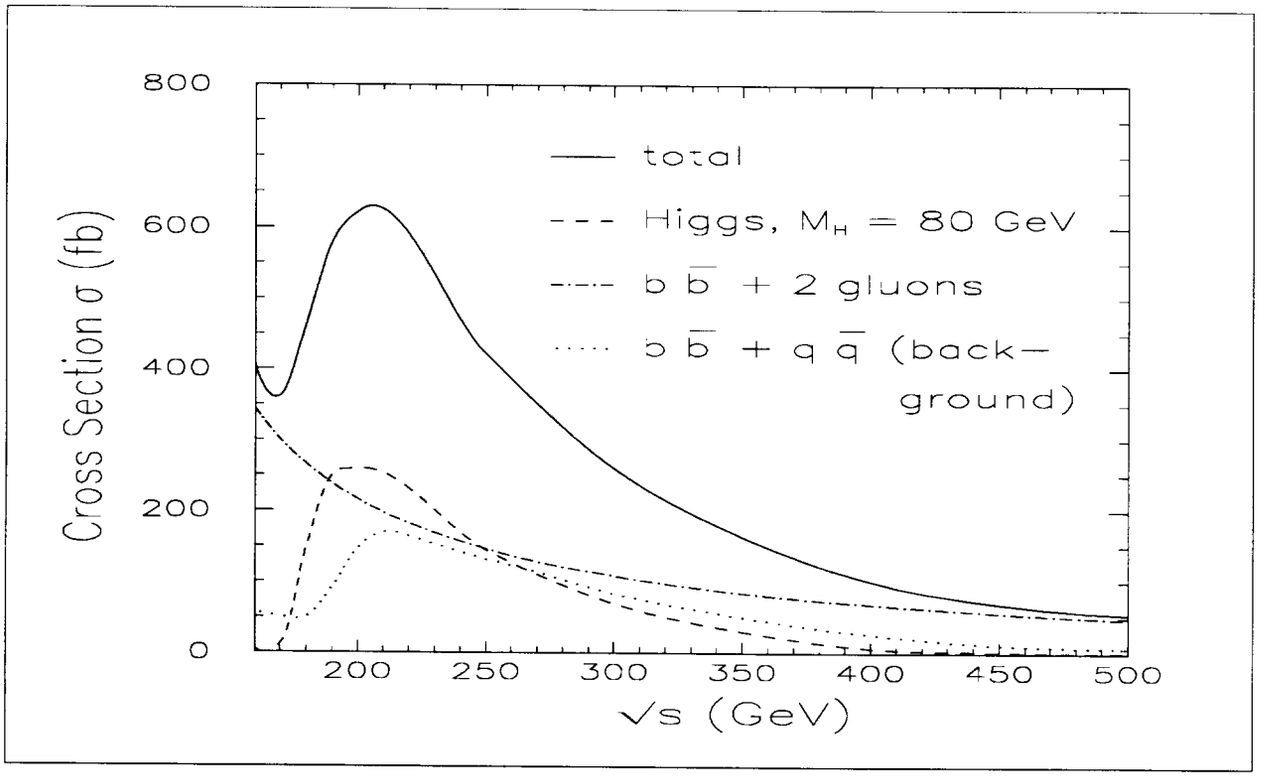

Figure 3: Cross sections for reactions (7) and (9), the background part of reaction (8) and the Higgsstrahlung off the Z boson as function of the cms energy, with $M_{ij} > 10$ GeV and $|\cos\Theta_{ij}| < 0.9$.

maximum at $\sqrt{s} \simeq M_Z + \sqrt{2}M_H$ and fall with $1/s$ at higher energies. It is also evident from Fig. 4 that at $\sqrt{s} > 300$ GeV cross sections for smaller Higgs masses are less than those with larger masses. This somewhat unexpected behaviour is due to our principal cuts (10).

According to these results one expects about 125 4-jet H^0 events (with $H^0 \longrightarrow b\bar{b}$ and $M_H = 80$ GeV) at $\sqrt{s} = 200$ GeV for an integrated luminosity of $\mathcal{L} = 500$ pb^{-1}. For a NLC at $\sqrt{s} = 300$ GeV and an integrated luminosity of 10 fb^{-1}, the prospects for Higgs detection and its analysis are quite good for a large range of Higgs masses: about 750 events are expected for $M_H = 80$ GeV and ~ 600 events for $M_H = 140$ GeV, see also ref. [22].

We would like to point out that in addition to the H^0 signal discussed so far there exist H^0Z diagrams, with $H^0 \longrightarrow q\bar{q}$ ($q = u, d, s$ or c) and $Z \longrightarrow b\bar{b}$ decays, and those of H^0 radiation off a b quark with subsequent $H^0 \longrightarrow q\bar{q}$ ($q \neq b$) decay, corresponding to the diagrams (K) respectively (L) and (M) in Fig. 1. These diagrams also feed the 4-jet topology with two identified b quarks as selected in our study. The corresponding rate is however found to be small, e.g. about 1 fb at $\sqrt{s} = 300$ GeV and $M_H = 140$ GeV, and essentially due to $H^0 \longrightarrow c\bar{c}$ decay. Since in this study only $H^0 \longrightarrow b\bar{b}$ events are considered to be a valid Higgs signature, all the other H^0 decays are added to the background. These events might however become relevant once the H^0 has been discovered,

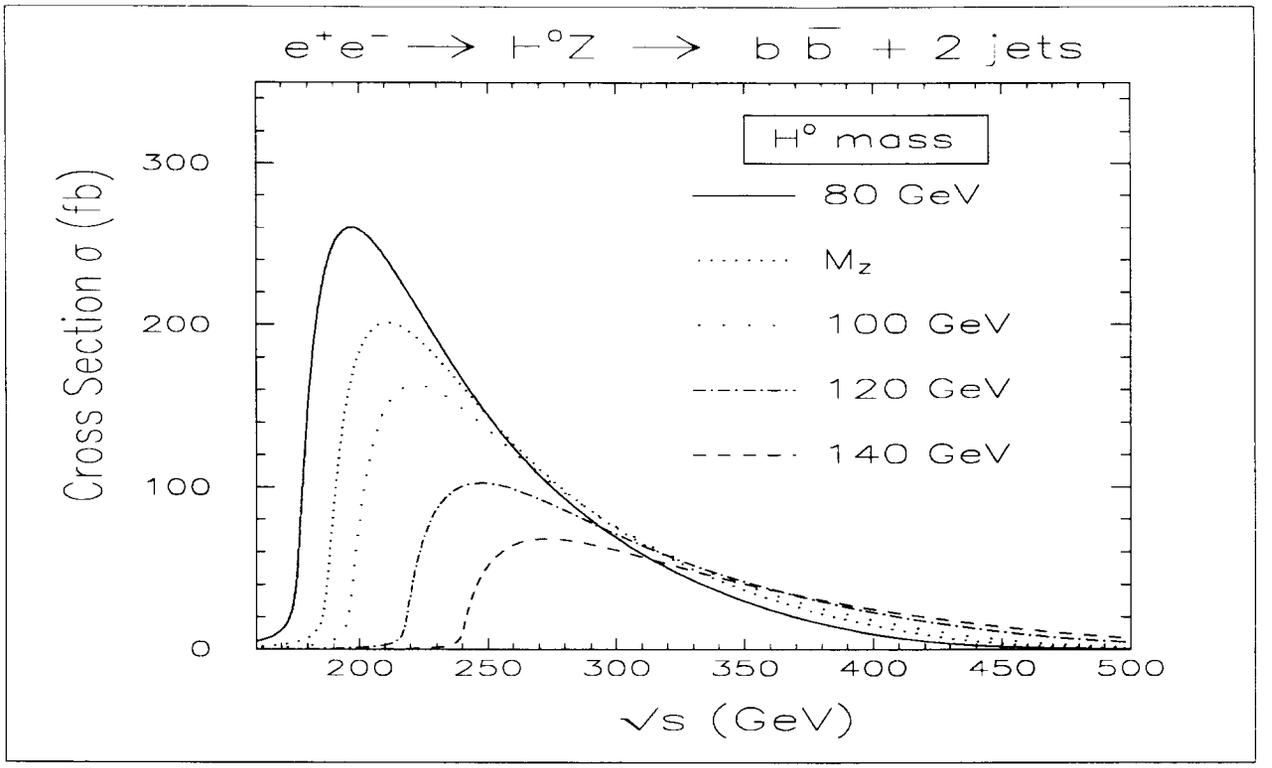

Figure 4: Higgs production cross sections as function of the cms energy for different Higgs masses, with $M_{ij} > 10$ GeV and $|\cos\Theta_{ij}| < 0.9$.

for obtaining further Higgs-fermion coupling information.

In Fig. 5 we present some H^0 event distributions as expected for $\sqrt{s} = 200$ GeV, $M_H = 80$ GeV and $\mathcal{L} = 500$ pb^{-1}, while Fig. 6 shows the analogous distributions for $\sqrt{s} = 300$ GeV, $M_H = 140$ GeV and $\mathcal{L} = 10$ fb^{-1}. In particular, we present in these figures the $b\bar{b}$ and 2-jet invariant mass distributions, the total $b\bar{b}$ energy and rapidity and the event sphericity distribution. Inspection of these spectra and their comparison with the corresponding background distributions may suggest appropriate cuts to remove most of the background while keeping the signal unaltered.

4 The background contributions

The two background contributions to process (7), $e^+e^- \longrightarrow b\bar{b}$ + 2 jets, are the non-Higgs part of reaction (8) with a $q\bar{q}$ pair in the final state, $e^+e^- \longrightarrow b\bar{b} + q\bar{q}$, and reaction (9) with two gluons produced, $e^+e^- \longrightarrow b\bar{b} + gg$. The cross sections for these processes are presented as a function of $\sqrt{s}$ in Fig. 3. In the following we will discuss these processes in more detail.

Reaction (8) involves, as shown in Fig.1, two kinds of diagrams: the pure electroweak (EW) diagrams (denoted with (D) to (Q)) and diagrams with internal gluon radiation (QCD) (the diagrams (R) to (U)). Interferences between

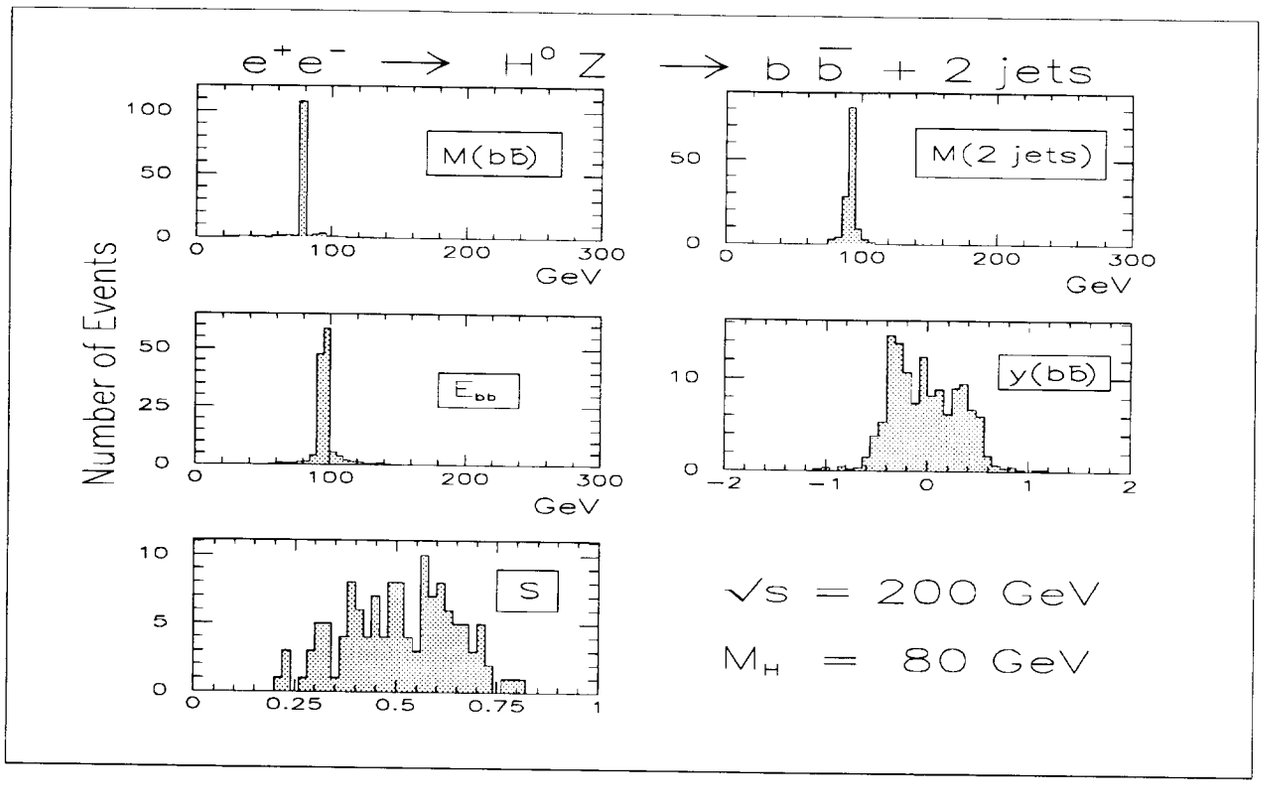

Figure 5: Event distributions for Higgs production ($M_H = 80$ GeV) as functions of the $b\bar{b}$ and 2-jet invariant masses, the $b\bar{b}$ energy and rapidity and the event sphericity at a cms energy of 200 GeV for an integrated luminosity of 500 pb^{-1}, with $M_{ij} > 10$ GeV and $|\cos\Theta_{ij}| < 0.9$.

both types do not occur as long as $q \neq b$ and $\bar{q} \neq \bar{b}$ because quark pairs originating from a gluon have an octet colour structure while those from the EW-part have a singlet colour structure. In the case of $q = b$ and $\bar{q} = \bar{b}$ production, interferences may occur, and they turned out to be very small; e.g. at $\sqrt{s} =$ 200 GeV they are -1.8 10^{-1} fb. Thus it is justified in all further calculations to add the EW and QCD contributions to reaction (8) incoherently. Their individual cross sections are presented in Fig. 7 as a function of $\sqrt{s}$, for three choices of the $q\bar{q}$ pair: $d\bar{d}$(or $s\bar{s}$), $u\bar{u}$(or $c\bar{c}$) and $b\bar{b}$. These cross sections are controlled by the onset of the two-body reaction $e^+e^- \longrightarrow ZZ$ in the energy range of LEPII. Other t-channel two-body processes like $e^+e^- \longrightarrow Z\gamma^*$ or $\gamma^*\gamma^*$ (with subsequent Z and γ^* decays into the corresponding quark pairs) were found to contribute with few percent only. Interferences within these t-channel reactions should however be taken into account, whereas interferences between the t-channel reactions corresponding to diagram (D) and all the s-channel diagrams of Fig. 1, are negligible; they are found to be in the order of 0.1 fb. This is qualitatively in agreement with the results found for the reaction $e^+e^- \longrightarrow b\bar{b}$ $\mu^+\mu^-$ [10]. The W pair production process, $e^+e^- \longrightarrow W^+W^- \longrightarrow (b\bar{q})(\bar{b}q)$, corresponding to diagrams (E) and (F) in Fig. 1, has also been calculated and found to be very small. At $\sqrt{s} = 200$ GeV for instance, its cross section is $\sim$4

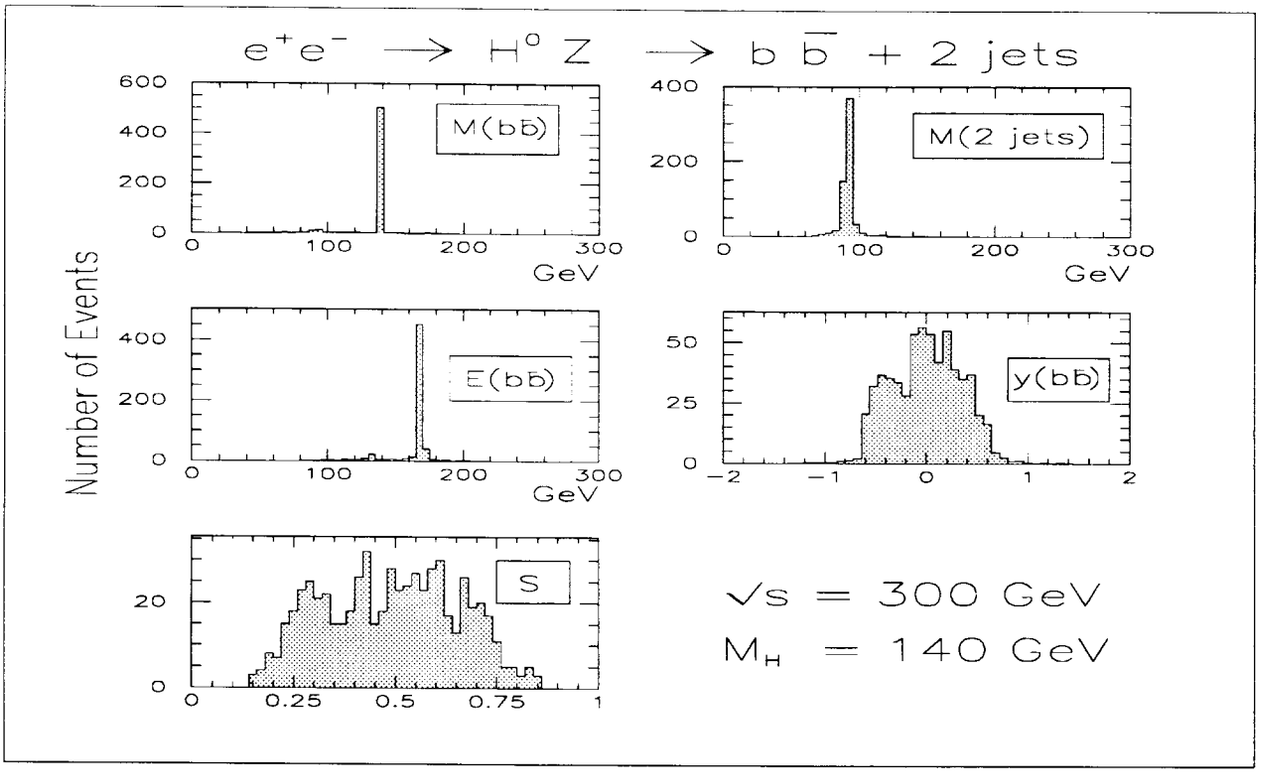

Figure 6: Event distributions for Higgs production ($M_H = 140$ GeV) as functions of the $b\bar{b}$ and 2-jet invariant masses, the $b\bar{b}$ energy and rapidity and the event sphericity at a cms energy of 300 GeV for an integrated luminosity of 10 fb^{-1}, with $M_{ij} > 10$ GeV and $|\cos\Theta_{ij}| < 0.9$.

10^{-6} pb. Thus, W pair production represents a negligible contribution to the background which is due to the small W-coupling to a b and lighter quarks. The 1-gluon QCD cross sections in Fig. 7 reveal a smooth $\sqrt{s}$ dependence and are significantly smaller than the EW values in the energy range $\sqrt{s} \simeq$ 200 - 400 GeV. This is first of all ascribed to the absence of a corresponding t-channel ZZ contribution and the strong influence of the principal cuts (10), applied from the beginning.

It is also evident from Fig. 7 that, within the EW cross sections, the $b\bar{b}$ production rate is about two times smaller than that in the case of $d(s)$ or $u(c)$ quarks. The reason is the existence of two identical $b\bar{b}$ quark pairs in the final state which leads to a suppression factor of 1/2. Some further small suppression of the $b\bar{b}$ + $b\bar{b}$ final state occurs from the larger b quark mass. The differences between the $u\bar{u}$ and $d\bar{d}$ cross sections as seen in Fig. 7, are due to different couplings of the Z-boson to the up and down quarks within the SM[1].

The other background reaction, $e^+e^- \longrightarrow b\bar{b} + gg$, either dominates the total background rate or is comparable to that of the process $e^+e^- \longrightarrow b\bar{b}$ + $q\bar{q}$ (Fig. 3), even after the application of the principal cuts (10). These

[1]Cross section differences between $d\bar{d}$ and $s\bar{s}$ (or $u\bar{u}$ and $c\bar{c}$) quark pair production were found to be very small and can be neglected.

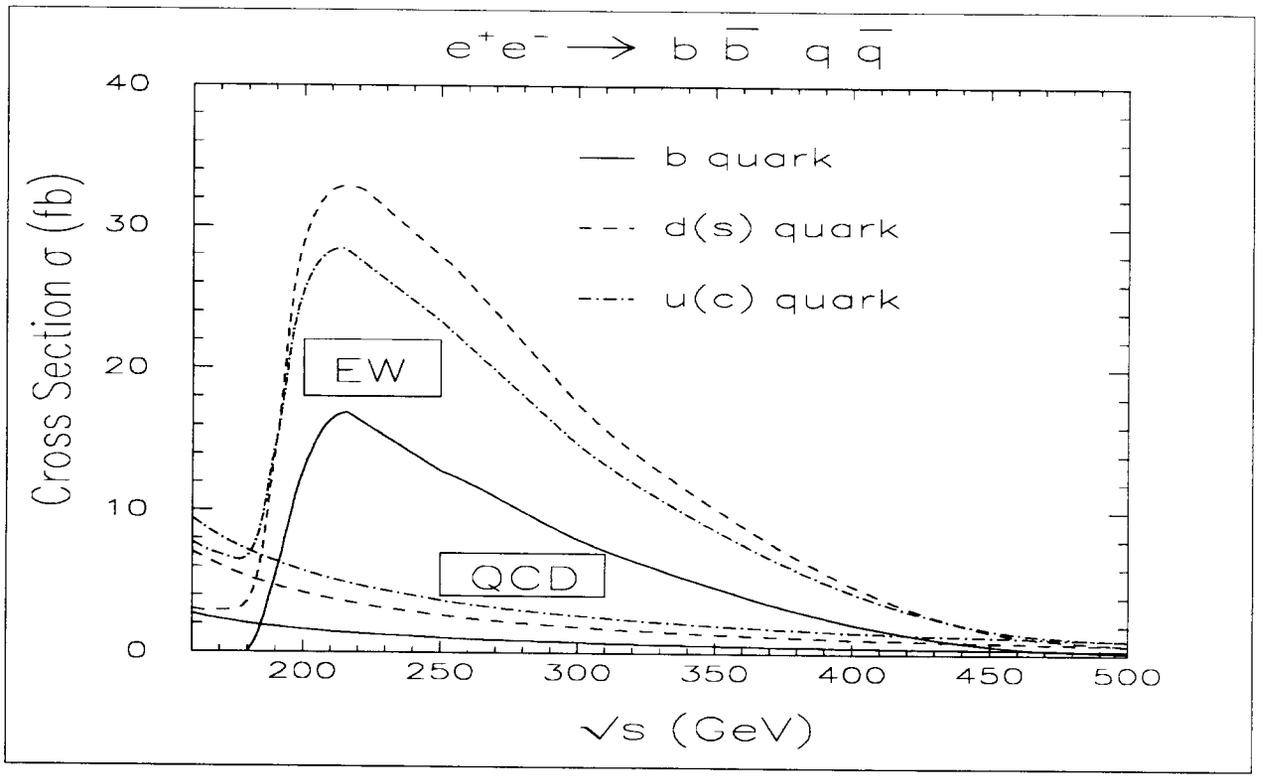

Figure 7: Background cross sections of pure electroweak nature (EW) and of internal gluon radiation (QCD) as function of the cms energy for three choices of the $q\bar{q}$ pair, $d\bar{d}$(or $s\bar{s}$), $u\bar{u}$(or $c\bar{c}$) and $b\bar{b}$, with $M_{ij} > 10$ GeV and $|\cos\Theta_{ij}| < 0.9$.

cuts are important not only to ensure a 4-jet final state topology but also to avoid threshold singularities in the invariant mass distribution of two massless gluons or two massless quarks and at zero-angle gluon radiation. It is worth emphasizing that changes of these cuts strongly influence the background cross section values.

In order to understand in more detail the behaviour of the main background sources discussed, we show in Figs. 8 and 9 the $b\bar{b}$ and 2-jet invariant mass distributions, the total $b\bar{b}$ energy and rapidity and the event sphericity distribution expected for $\sqrt{s} = 200$ GeV, $M_H = 80$ GeV and $\mathcal{L} = 500$ fb^{-1}, reprectively, for $\sqrt{s} = 300$ GeV, $M_H = 140$ GeV and $\mathcal{L} = 10$ fb^{-1}. These distributions may be helpful to define cuts in order to remove most of the background while retaining the H^0 signal.

5 The extraction of the H^0 signal

In the previous sections we have discussed in some detail the behaviour of the H^0 and the background events. H^0 events were found to be essentially produced from the Higgsstrahlung off the Z boson (diagram (A) in Fig. 1); all other possibilities turned out to be negligible. It is therefore inevitable to

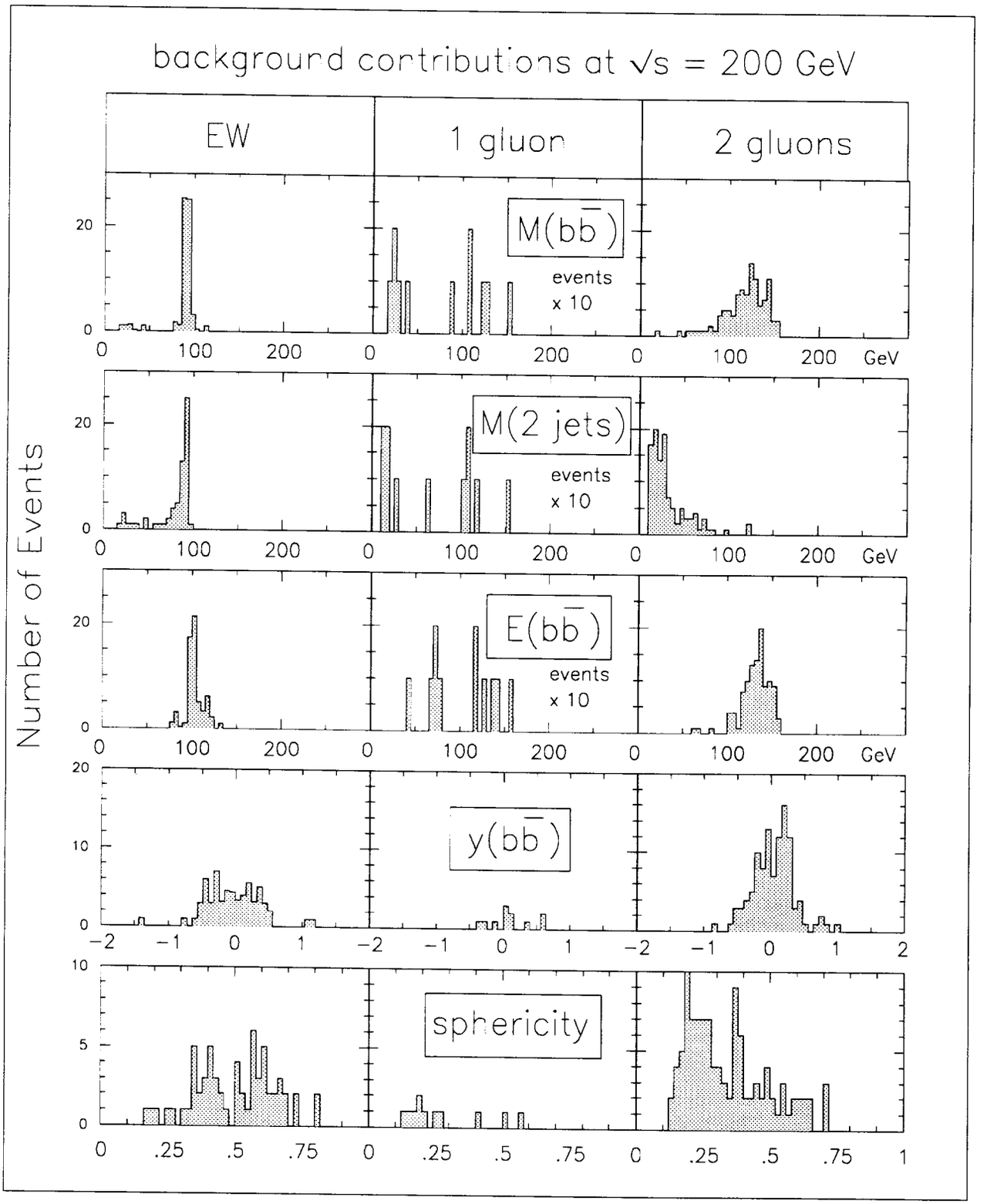

Figure 8: Event distributions for the electroweak, the internal gluon and 2 gluon background contributions as functions of the $b\bar{b}$ and 2-jet invariant masses, the $b\bar{b}$ energy and rapidity and the event sphericity at a cms energy of 200 GeV for an integrated luminosity of 500 pb^{-1}, with $M_{ij} > 10$ GeV and $|\cos\Theta_{ij}| < 0.9$.

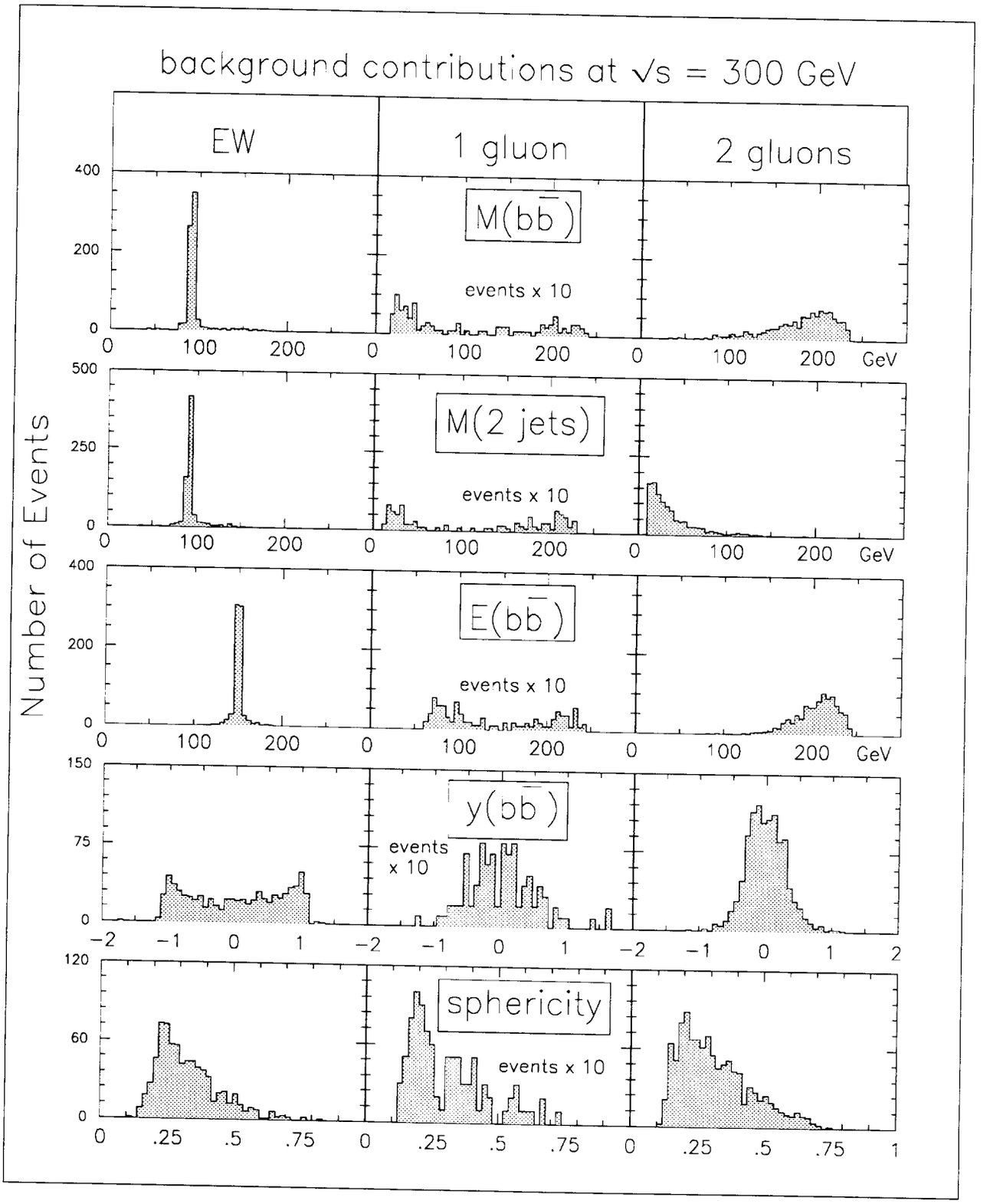

Figure 9: Event distributions for the electroweak, the internal gluon and 2 gluon background contributions as functions of the $b\bar{b}$ and 2-jet invariant masses, the $b\bar{b}$ energy and rapidity and the event sphericity at a cms energy of 300 GeV for an integrated luminosity of 10 fb^{-1}, with $M_{ij} > 10$ GeV and $|\cos\Theta_{ij}| < 0.9$.

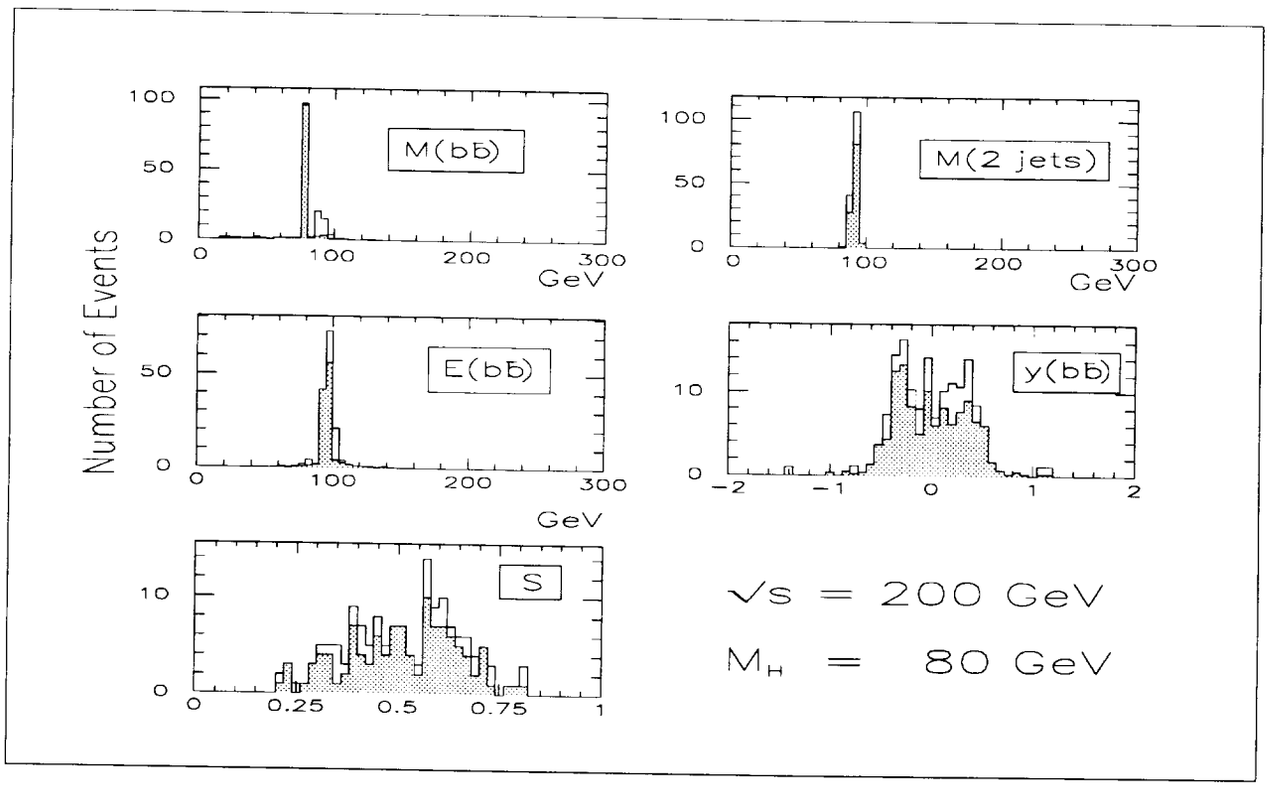

Figure 10: Event distributions for the reaction $e^+e^- \to b\bar{b}$ + 2 jets and the Higgs events (shaded) with the condition $M(2\text{ jets}) = M_Z \pm 5$ GeV as functions of the $b\bar{b}$ energy and rapidity and the event sphericity at a cms energy of 200 GeV and $M_H = 80$ GeV for an integrated luminosity of 500 pb^{-1}, with $M_{ij} > 10$ GeV and $|\cos\Theta_{ij}| < 0.9$.

require that the 2-jet invariant mass recoiling off the H^0 is equal to M_Z (within the range of e.g. $\pm$ 5 GeV). Figs. 10 and 11 show for such selected events the distributions of Figs. 8 or 9 for $\sqrt{s} = 200$ GeV, $M_H = 80$ GeV and $\mathcal{L} = 500$ fb^{-1}, respectively, $\sqrt{s} = 300$ GeV, $M_H = 140$ GeV and $\mathcal{L} = 10$ pb^{-1}. The shaded spectra in these figures correspond to the H^0 events. It is evident that at $\sqrt{s} = 200$ GeV a simple M_Z-cut removes most of the background, and an inspection of the $b\bar{b}$ invariant mass distribution reveales that the Higgs signal can be extracted practically background-free.

At $\sqrt{s} = 300$ GeV, about 68 % of the total background is removed by the M_Z-cut, and again, the $M(b\bar{b})$ spectrum shows a clear H^0 peak, with negligible 0.5% background underneath the signal. In both cases, almost all H^0events are retained for further analyses.

It is however worth emphasizing that in practice non-4-jet events and some b-tagging inefficiency may fake 4-jet events with two b-jets involved. To remove such background, variables like the total $b\bar{b}$ energy, the rapidity and the event sphericity are probably very helpful [6], and as seen in Fig. 11, they are also useful in suppressing genuine 4-jet background events with a $b\bar{b}$ quark pair in the final state.

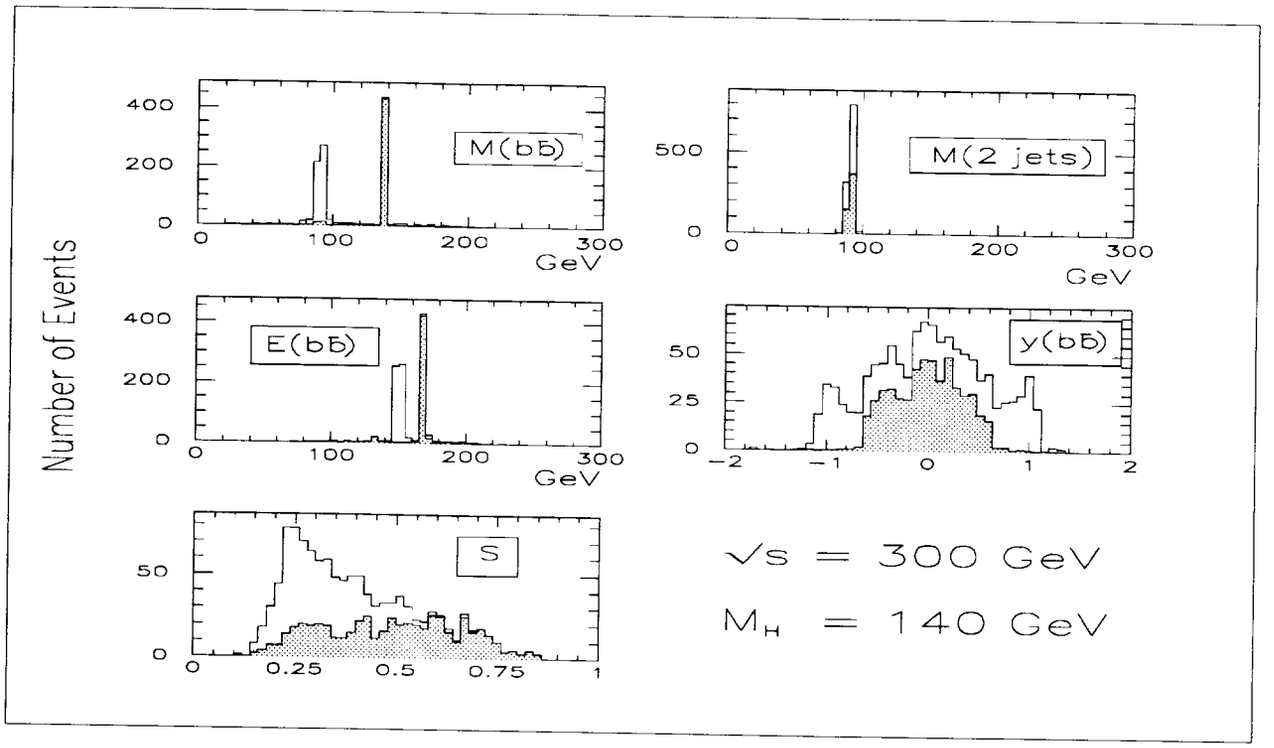

Figure 11: Event distributions for the reaction $e^+e^- \to b\bar{b}$ + 2 jets and the Higgs events (shaded) with the condition $M(2\text{ jets}) = M_Z \pm 5$ GeV as functions of the $b\bar{b}$ energy and rapidity and the event sphericity at a cms energy of 300 GeV and $M_H = 140$ GeV for an integrated luminosity of 10 fb^{-1}, with $M_{ij} > 10$ GeV and $|\cos\Theta_{ij}| < 0.9$.

6 Summary and conclusions

We have computed the exact matrix elements, at tree-level, for the reaction $e^+e^- \longrightarrow b\bar{b}$ + 2 jets at LEPII and NLC energies. The 2-jet system is a $q\bar{q}$ system (with $q = u, d, s, c$ and b) or consists of two gluons. In order to impose a 4-jet $b\bar{b}$ final state topology we only accepted events having invariant masses of any pair of partons $M_{ij} > 10$ GeV with an opening angle $|\cos\Theta_{ij}| < 0.9$, and assumed a perfect b quark identification.

Concerning the H^0 signal in its dominant decay mode $H^0 \longrightarrow b\bar{b}$ for intermediate Higgs masses, only Higgsstrahlung off the Z boson is important. Other mechanisms and interference terms were found to be negligible. It is shown that $\sqrt{s} \sim 300$ GeV is a very well suited energy for Higgs detection, for H^0 masses in the range of about 90 to 140 GeV, both from the point of view of rates as well as for the signal/background ratio.

The background is dominated by the 2-gluon contribution for $\sqrt{s} < 180$ GeV and also at NLC energies. Its relative amount is strongly determined by the cuts mentioned above. Most of the $b\bar{b}\,q\bar{q}$ background comes from the two-body reaction $e^+e^- \longrightarrow ZZ$. It reaches a maximum close to 200 GeV and shows a $1/s$ fall-off at higher energies. The internal gluon radiation component, the QCD part of the reaction $e^+e^- \longrightarrow b\bar{b}$ + $q\bar{q}$, dominates at low energies

and decreases with growing $\sqrt{s}$ such that it becomes comparable to the pure electroweak $b\bar{b}$ $q\bar{q}$ background close to 500 GeV. W^+W^- production is completely negligible in the 4-fermion final states considered.

Several event distributions, calculated for reasonable integrated luminosities, both for the H^0 signal and the most important background contributions, are presented for $\sqrt{s}$= 200 GeV and $M_H = 80$ GeV as well as for $\sqrt{s}$= 300 GeV and $M_H = 140$ GeV. By means of appropriate cuts in the variables suggested it should be possible to remove most of the background events while retaining the H^0 signal. Experience from LEP [6] already indicates that these variables are also very helpful to suppress faked 4-jet background events which might be dominant in realistic Higgs searches.

Acknowledgements

We would like to thank V. A. Ilyin and A. E. Pukhov for many discussions and the help with CompHEP calculations. E.B. and S. Sh. would like to thank P. Söding for his interest and support and are grateful to DESY-IfH Zeuthen for the kind hospitality. The work has partially been supported by the ISF grant No. M9B000 and by the INTAS grant INTAS-93-1180.

References

[1] S. L. Glashow, Nucl. Phys. **22** (1961) 579;
S. Weinberg, Phys. Rev. Lett. **19** (1967) 1264;
A. Salam, Elementary Particle Theory, ed. by N. Svartholm, Stockholm (1968),p. 367.

[2] F. Richard, preprint LAL 94-50 (September 1994), talk given at the 27^{th} Int. Conf. on High Energy Physics, Glasgow, July, 20-27^{th} 1994.

[3] J. F. Gunion, H. E. Haber, G. Kane and S. Dawson, The Higgs Hunter's Guide, Addison-Wesley 1990;
H. E. Haber, Physics and Experiments with Linear Colliders, ed. by R. Orava, P. Eerola and M. Nordberg, World Scientific Publishing Co.,1992,p. 235;
A. Djouadi, D. Haidt and P. M. Zerwas, Proc. of the Workshop - Munich, Annecy, Hamburg, 1991, ed. by P. M. Zerwas, DESY Report 92-123A, p. 1;
A. Djouadi, D. Haidt, B. A. Kniehl, B. Mele and P. M. Zerwas, Proc. of the Workshop - Munich, Annecy, Hamburg, 1991, ed. by P. M. Zerwas, DESY Report 92-123A, p. 11.

[4] J. Ellis, M.K. Gaillard and D.V. Nanopoulos, Nucl. Phys. **B106** (1976) 292;
J.D. Bjorken, Proc. of Summer Institute on Particle Physics, SLAC Report 198(1976).

[5] D.R.T. Jones and S.T. Petkov, Phys. Lett. **B84** (1979) 440;
R.N. Cahn and S. Dawson Phys. Lett. **B136** (1984) 196.

[6] S.L. Wu et. al. preprint CERN-EP/87-40.

[7] S. Komamiya, Physics and Experiments with Linear Colliders, ed. by R. Orava, P. Eerola and M. Nordberg, World Scientific Publishing Co.,1992,p. 277.

[8] P. Janot, preprint LAL 93-38 (July 1993), talk given at the Second Int. Workshop on Physics and Experiments with Linear e^+e^- Collider, Waikoloa, Hawaii, 1993.

[9] V. Barger, K. Cheung, A. Djouadi, B.A. Kniehl and P. M. Zerwas, Phys. Rev. **D49** (1994) 79.

[10] E. Boos, M. Sachwitz, H.J. Schreiber and S. Shichanin, Z. Phys. **C61** (1994) 675;
D. Bardin, A. Leike and T. Riemann, preprint CERN-TH. 7305/94.

[11] E. Boos, M. Sachwitz, H.J. Schreiber and S. Shichanin, preprint DESY 93-183, accepted for publication in Int. Journal of Mod. Phys. A.

[12] M. Dubinin, V. Edneral, Y. Kurihara and Y. Shimizu, Phys. Lett. **B329** (1994) 379.

[13] E. Boos, M. Sachwitz, H.J. Schreiber and S. Shichanin, Z. Phys. **C64** (1994) 391.

[14] e.g. A. Ballestrero, E. Maina and S. Moretti, Nucl. Phys. **B415** (1994) 265, and references therein.

[15] F.A. Berends, R. Pittau and R. Kleiss, Nucl. Phys. **B424** (1994) 308.

[16] D. Bardin, M. Bilenky, A. Leike and T. Riemann, preprint DESY 94-185.

[17] D. Bardin, M. Bilenky, D. Lehner, A. Olchevski and T. Riemann, preprint CERN-TH.-7295/94;
D. Bardin, M. Bilenky, A. Olchevski and T. Riemann, Phys. Lett. **B308** (1993) 403.

[18] R. Pittau, Phys. Lett. **B335** (1994) 490.

[19] E. E. Boos et al. Proc. of the XXVIth Recontre de Moriond, ed. by J. Tran Than Van, Edition Frontiers, 1991, p. 501;
E. E. Boos et al., Proc. of the Second Int. Workshop on Software Engineering, ed. by D. Perred-Gallix, World Scientific, 1992, p. 665;
E. E. Boos et al., preprint KEK 92-47, 1992.

[20] S. Kawabata, Comp. Phys. Commun. **41** (1986) 127.

[21] V.A. Ilyin and A.E. Pukhov, preprint in preparation.

[22] P. Grosse-Wiesmann, D. Haidt and H. J. Schreiber, Proc. of the Workshop - Munich, Annecy, Hamburg, 1991, ed. by P. M. Zerwas, DESY Report 92-123A, p. 37.